GENERALIZED BINOMIAL TRANSFORM APPLIED TO THE DIVERGENT SERIES

Hirofumi Yamada

Division of Mathematics and Science, Chiba Institute of Technology
Shibazono 2-1-1, Narashino, Chiba 275-0023, Japan

(Received February 23, 2016; accepted October 27, 2016)

The divergent series for a function defined through Lapalce integral and the ground state energy of the quartic anharmonic oscillator to large orders are studied to test the generalized binomial transform which is the renamed version of δ expansion proposed recently. We show that, by the use of the generalized binomial transform, the values of functions in the limit of zero of an argument are approximately computable from the series expansion around the infinity of the same argument. In the Laplace integral, we investigate the subject in detail with the aid of Mellin transform. In the anharmonic oscillator, we compute the strong coupling limit of the ground state energy and the expansion coefficients at strong coupling from the weak coupling perturbation series. The obtained result is compared with that of the linear delta expansion.

DOI:10.5506/APhysPolB.47.2413

1. Introduction

The δ expansion proposed in Ref. [1] has been considered so far on the discretized background. In all applications of the method, the expansion in terms of the basic parameter has a finite radius of convergence such as the strong coupling expansion in the field theoretic models on lattice and high temperature expansion in magnetic systems [2, 3]. The existence of the non-zero convergence radius plays an important role in the application of the δ expansion. The aim of this paper is to investigate whether the method is effective in asymptotic series appearing in perturbation expansion. Here, we will apply the method to two models, a mathematical function defined through Laplace integral and the quantum mechanical anharmonic oscillator in which we focus on the computation of the ground state energy at strong coupling from the weak coupling perturbation theory to large perturbative orders.

Before the argument, to avoid possible confusion, we would like to rename the "δ expansion" used in [1] to the "generalized binomial transform" for the following reasons: The anharmonic oscillator can be viewed as the Euclidean 1-dimensional ϕ^4 field theory. The Hamiltonian then reads

$$H = \frac{1}{2}\left(\frac{\partial\phi}{\partial q}\right)^2 + \frac{m^2}{2}\phi^2 + \lambda\phi^4\,, \tag{1.1}$$

where we denoted the Euclidean time coordinate by q.

The nonlinear interaction is controlled by the coupling constant λ and the unperturbed current mass is given by m. The perturbation theory provides an expansion of any physical quantity in λ. Due to the mass dimension 3 carried by the coupling constant, expansion in λ is actually the expansion in dimensionless parameter λ/m^3. Thus, it is apparent that the perturbative expansion is almost equivalent with the inverse-mass expansion. There exists a novel computational technique called "linear delta (δ) expansion", "optimized perturbation theory" or "variational perturbation theory" [4]. Also the "order dependent mapping" [5] method, which includes "linear delta (δ) expansion" in a specific fixing of the mapping, shares a similar feature. In the anharmonic oscillator, the "δ expansion" proposed in [1] has similarities to these techniques. The conventional linear delta expansion introduces δ as the interpolating parameter by the substitutions $m^2 \to m^2(1-\delta)$ and $\lambda \to \lambda\delta$. The Hamiltonian to start with is

$$H(\delta) = \frac{1}{2}\left(\frac{\partial\phi}{\partial q}\right)^2 + \frac{m^2}{2}\phi^2 + \delta\left(-\frac{m^2}{2}\phi^2 + \lambda\phi^4\right)\,. \tag{1.2}$$

Notice that the system at $\delta = 0$ reduces to the free massive oscillator and the system at $\delta = 1$ to the massless anharmonic oscillator (pure anharmonic oscillator). One then regards $H(0) = \frac{1}{2}(\partial\phi/\partial q)^2 + (m^2/2)\phi^2$ as the unperturbed part and expands the perturbation $\delta[-(m^2/2)\phi^2 + \lambda\phi^4]$ as the power series in δ. The result is understood as the perturbative one of the interpolated system with the mass $m^2(1-\delta)$ and the coupling constant $\delta\lambda$. Then, setting $\delta = 1$, one may obtain nontrivial and effective estimates of physical observables in the massless limit (or the strong coupling limit). The literature on the method is quite extensive, see, for example, paper [4] and references therein. For the application of linear delta expansion on the lattice, see [6].

The "δ expansion" proposed in Ref. [1] has been derived in the similar technique. Suppose that $f(m^2)$ be given as the truncated series in $1/m^2$ to the order N,

$$f_N\left(m^2\right) = \sum_{n=0}^{N} a_n \left(\frac{1}{m^2}\right)^n\,. \tag{1.3}$$

By the rescaling of the argument $m^2 = (1-\delta)/t$, expanding $f_N((1-\delta)/t)$ in δ to the relevant order and setting $\delta = 1$, one obtains the δ expansion of f as the function of t (see (1.4)). This technique is first used on the lattice as a tool of dilatation of the continuum scaling region, where the argument is basically related to the lattice spacing. On the other hand, the linear delta expansion is stemmed from the interpolation of two different systems. Though the two tools share similar features and sometimes produce the same results, they differ in the underlying concept and specific details, in particular, when applied to physical systems on the lattice. This is the main reason of renaming the "δ expansion" to "generalized binomial transform" or simply in short "binomial transform".

It would be in order to review briefly the generalized binomial transform: In typical cases, the generalized binomial transform acts on the simple truncated power series (1.3) as

$$\mathcal{B}_N\left[f_N\left(m^2\right)\right] = \sum_{n=0}^{N} a_n \binom{N}{n} t^n \,. \tag{1.4}$$

That is, the coefficient a_n in original series is multiplied by the binomial factor

$$\binom{N}{n} = \frac{N!}{n!(N-n)!} \,, \qquad (0 \le n \le N) \,. \tag{1.5}$$

Thus, the binomial transform denoted by $\mathcal{B}_N$ is dependent on the perturbative order N. For the sake of notational simplicity, we also use "bar" to imply the transform

$$\mathcal{B}_N\left[f_N\left(m^2\right)\right] := \bar{f}_N(t) \,. \tag{1.6}$$

At first sight, one may feel difficulty in understanding the effectivity of $\bar{f}_N(t)$ in extracting the quantities, the limit $\lim_{m\to 0} f(m^2) = f(0)$ or the critical exponent when divergent in power-like manner as $m \to 0$. Though $\bar{f}_N(t)$ is just a polynomial in t, we found in some physics models that the asymptotic behavior of $f(m^2)$ as $m \to 0$ is observable in $\bar{f}_N(t)$ at *non-large t region* and the marking quantities (the limit and critical exponents) can be estimated. For instance, in the square Ising model at temperature $1/\beta$, β is expressed as a function of the mass-like parameter M which is roughly the inverse of the square of the correlation length (M is composed by the magnetic susceptibility χ and the second moment μ_2 as $M = 4\chi/\mu_2$). The effective region of $\mathcal{B}_N[\beta(M)] = \bar{\beta}_N(t)$ in the $N \to \infty$ is numerically assured to be $0 < t < 0.25$ [2] over which the function exhibits an extremely flat plateau and the inverse critical temperature β_c is indicated at the stationary or almost stationary point of the function $\bar{\beta}_N(t)$. For convergent series, it is

implied that the limit $\lim_{N\to\infty}\mathcal{B}_N[f_N]$ is constant over $0 < t < t_c$ for a certain t_c and the function in the $N \to \infty$ limit has the shape like the step function with the finite range $(0, t_c)$.

Turning to the anharmonic oscillator, we deal with the perturbative expansion in powers of the coupling constant λ. Then, remembering that the ground state energy $E(m, \lambda)$ has an asymptotic expansion in λ/m^3 with alternate signs, there are two crucial differences compared to the Ising case and 2D large N vector model discussed in Refs. [1–3]. The first is that the expansion parameter has fractional powers of $1/m^2$ such as $(1/m^2)^{-1/2}$, $(1/m^2)^{5/2}$ and so on. To handle these terms, we use the generalized binomial factor

$$\binom{N}{s} = \frac{\Gamma(N+1)}{\Gamma(s+1)\Gamma(N-s+1)}\,, \tag{1.7}$$

where s is real or complex when the extension is convenient or necessary, and the transformation rule is given by

$$\mathcal{B}_N\left[M^{-s}\right] = \binom{N}{s} t^s\,, \qquad M = m^2\,. \tag{1.8}$$

As we shall see in the next section, this rule is suitable when the function $f(M)$ of interest allows Mellin transform representation.

Second, as aforementioned, the original series has zero convergence radius and it is unclear at all whether the generalized binomial transform effectively works as before. In this paper, we will demonstrate that a careful use of the principle of minimum sensitivity (PMS) [7] provides an accurate sequence of estimates to large enough orders.

This paper is organized as follows: In the second section, we apply the binomial transform to a mathematical function which allows divergent expansion such that $(1/M) - 2!(1/M)^2 + 3!(1/M)^3 - \ldots$ and investigate in detail the computation of the limit $M \to 0$ from the divergent series expanded at $M = \infty$, the opposite end point of the argument contained in the range $(0, \infty)$. The technique of Mellin transform representation is introduced to make the analysis transparent. From this example, one can gain concrete feeling of how binomial transform works. In the third section, we investigate the application of the binomial transform to the anharmonic oscillator. We first review weak coupling perturbation expansion and consider its transform. The linear delta expansion is also mentioned and the difference is explained. Explicit estimation will be worked out to the order of $N = 300$. The sequence of the estimates indicates the strong evidence of the convergence to the most precise value to date, even though the region "effective" in the estimation shrinks as the order grows. Also presented is the computation of the strong coupling coefficients and the result is

compared with that from the conventional linear delta expansion. The binomial transform related to the dilatation of the region around $\lambda = \infty$ is finally investigated. The last section is devoted to the concluding remarks.

2. A Laplace integral

2.1. Mellin transform

In the use of transformation rule (1.8) to the closed form of function, Mellin transform plays an important role. Given a function f as the argument M, the representation through Mellin transform reads

$$f(M) = \int_{c-i\infty}^{c+i\infty} \frac{\mathrm{d}s}{2\pi i} M^{-s} \varphi(s)\,, \tag{2.1}$$

where

$$\varphi(s) = \int_0^\infty \mathrm{d}M\, M^{s-1} f(M)\,. \tag{2.2}$$

In (2.1), the integration contour in the complex s-plane is taken as the vertical one passing through $c \in \mathbb{R}$ and it is assumed that the integral (2.1) exists in a certain vertical strip including the point $(c, 0)$.

The expansion of $f(M)$ at small M is given by the deformation of the contour to the left half-plane, by which residues at supposed poles leave the required series. As well, the expansion in $1/M$ is obtained by the deformation of the contour to the right half-plane.

When the Mellin transform representation is available, the generalized binomial transform is easy to implement. We find the result from (1.8) that

$$\begin{aligned} \bar{f}(t) &= \int_{c-i\infty}^{c+i\infty} \frac{\mathrm{d}s}{2\pi i} \mathcal{B}_N[M^{-s}]\varphi(s) \\ &= \int_{c-i\infty}^{c+i\infty} \frac{\mathrm{d}s}{2\pi i} \frac{\Gamma(N+1)}{\Gamma(s+1)\Gamma(N-s+1)} t^s \varphi(s)\,. \end{aligned} \tag{2.3}$$

The kernel changes from $\varphi(s)$ to $\frac{\Gamma(N+1)}{\Gamma(s+1)\Gamma(N-s+1)}\varphi(s)$. Deformation of the contour to the left half-plane gives the expansion of $\bar{f}(t)$ in $1/t$. Thus, the large M behavior of $f(M)$ corresponds to the small t behavior of $\bar{f}(t)$. If $\varphi(s)$ has single pole at $s = -L$ for positive integer L, expansion at small M has the term M^L. In contrast, for $\bar{f}(t)$, the corresponding t^{-L} term is

absent since then, the singularity is canceled by $1/\Gamma(s+1)$. If $\varphi(s)$ has double poles at $s=-L$, then there appears $M^L \log M$ in $f(M)$, but for $\bar{f}(t)$ just a power-like term t^L remains and the associated residue becomes

$$\frac{(-1)^{L+1}\Gamma(N+1)\Gamma(L)}{\Gamma(N+L+1)}\varphi_{-2}\,, \tag{2.4}$$

where the expansion $\varphi(s)=\varphi_{-2}/(s+L)^2+\ldots$ is supposed. It is crucial to note that the residue tends to vanish as $N^{-L}\varphi_{-2}$ as $N\to\infty$. Surviving term is the residue at $s=0$ only, provided the pole is surrounded in the contour deformation.

2.2. Generalized binomial transform applied to divergent expansion

Let us consider the mathematical function for $M>0$ defined through the Laplace integral given by

$$f(M)=M\int_0^\infty \frac{\omega\, e^{-M\omega}}{1+\omega}\mathrm{d}\omega\,. \tag{2.5}$$

From the well-known result of Mellin transform,

$$e^{-M\omega}=\int_{c-i\infty}^{c+i\infty}\frac{\mathrm{d}s}{2\pi i}(M\omega)^{-s}\Gamma(s)\,,\qquad \Re[s]>0\,, \tag{2.6}$$

we obtain the following representation

$$f(M)=\int_{c-i\infty}^{c+i\infty}\frac{\mathrm{d}s}{2\pi i}M^{1-s}\Gamma(s)\Gamma(s-1)\Gamma(2-s)\,, \tag{2.7}$$

where s must obey $1<\Re[s]<2$. The integrand has double poles at $s=1,0,-1,-2,\ldots$ and single poles at $s=2,3,\ldots$ By the deformation of the integration contour to the left or the right, one obtains the series expansion in M or $1/M$, respectively. Due to the double multiplicity of poles, the single power of the logarithm appears in expansion in M. The result reads from the residue computation that

$$f(M)=1+M\left(\log M+\gamma_{\mathrm{E}}\right)+O\left(M^2\log M\right)\,, \tag{2.8}$$

where γ_{E} denotes Euler–Mascheroni constant. The appearance of logarithm indicates the fact that the origin $M=0$ is a branch point. This is understood

by circulating the integration contour on the complex ω-plane. One then finds that the origin is a branch point and a circulation around the origin creates $2\pi i M e^M$, proving $f(M)$ be a multi-valued function.

We notice that $\lim_{M\to+0} f(M) = 1$ is given by the residue at $s = 1$ and the pole $s = 1$ is the first pole one encounters in the contour deformation to the left. On the other hand, $1/M$ expansion reads

$$f(M) = \frac{1!}{M} - \frac{2!}{M^2} + \frac{3!}{M^3} - \dots \tag{2.9}$$

This series is divergent and deriving the asymptotic behavior of $f(M)$ at small enough M requires a special technique such as the Bore transform. We would like to show that the binomial transform converts the $1/M$ series into the series from which $f(0)$ can be approximately computable, even when the series is truncated at a given finite order.

The operation of the binomial transform is straightforward. We find from (1.8) and (2.7) that

$$\bar{f}(t) = N! \int_{c-i\infty}^{c+i\infty} \frac{\mathrm{d}s}{2\pi i} \frac{\Gamma(s-1)\Gamma(2-s)}{\Gamma(N-s+2)} t^{s-1} . \tag{2.10}$$

The double poles of $f(M)$ at $s = 0, -1, -2, \dots$ have turned into the single poles and the expansion around $t = \infty$ becomes an infinite series without log. The poles at $s = N+2, N+3, \dots$ have disappeared due to the appearance of $1/\Gamma(N-s+2)$. Thus, the series expansion in t becomes a polynomial to the order N. Then

$$\bar{f}(t) = \sum_{k=1}^{N} \binom{N}{k} k!(-t)^k + R_N(t) , \tag{2.11}$$

where the function $R_N(t)$ represents the contribution from the deformed upward contour crossing at the positive real axis at some point located to the right of the largest pole $s = N+1$. In realistic physical application, one does not have complete information and suffices truncated series to the order N. Thus, we neglect the residual contribution R_N and keep only the polynomial denoted by $\bar{f}_N(t)$

$$\bar{f}_N(t) = \sum_{k=1}^{N} \binom{N}{k} k!(-t)^k = N! \sum_{k=1}^{N} \frac{(-t)^k}{(N-k)!} . \tag{2.12}$$

For large t, gathering all residues of the poles $s = 1, 0, -1, -2, \dots$, we obtain

$$\bar{f}(t) = \sum_{k=0}^{\infty} \frac{(-1)^k}{(N+1)\dots(N+k)t^k} = N! \sum_{k=0}^{\infty} \frac{(-1)^k}{(N+k)!t^k} . \tag{2.13}$$

This is the expansion around $t = \infty$ and manifests $\bar{f}(t)$ to be an entire function in the complex $1/t$-plane. The function $\bar{f}(t)$ is single valued with no cut. It is a crucial point here that all the coefficients except the one for the leading term tend to zero when $N \to \infty$. That is, $\bar{f}(t)$ tends to a uniform function

$$\lim_{N\to\infty} \bar{f}(t) = 1\,, \qquad 0 < t < \infty\,. \tag{2.14}$$

In the contour deformation, the pole one first encounters is $s = 1$ and the residue equals to 1. This is the limit $\bar{f}(\infty)$. The agreement of $f(0)$ and $\bar{f}(\infty)$ is not accidental because the residues at $s = 1$ are kept equal with each other by the generalized binomial transform (by which $\Gamma(N+1)/\{\Gamma(s)\Gamma(N-s+2)\}$, which is equal to 1 at $s = 1$, is created in the integrand). The function $\bar{f}(t)$ can be written as

$$\bar{f}(t) = N!\left[(-t)^N e^{-1/t} + \sum_{k=1}^{N} \frac{(-t)^k}{(N-k)!}\right]. \tag{2.15}$$

One can see that the second part agrees with $\bar{f}_N(t)$. The first term has the essential singularity at $t = 0$ and this is seen only in the deformation of the contour to the left plane. The term does not allow expansion in t and corresponds to $R_N(t)$, and leads us to understand that $\bar{f}(t)$ expressed in (2.13) and (2.15) provides the exact result of generalized binomial transform of $f(M)$ (contribution from the infinitely remote half-circle in the left half-plane disappears).

2.3. Reduction of corrections to the asymptotic scaling

Now, the point is whether $\bar{f}_N(t)$ to a given order N is useful or not to simulate the dominant or leading behavior of $\bar{f}(t)$ at large enough t. This is where the physics problems frequently arise. By the numerical study of $\bar{f}_N(t)$, we find that the transformed series shows the improved behavior compared to the original truncated series of $f(M)$. But the improvement is not sufficient and the estimation of $f(0) = \bar{f}(\infty)$ is not so good even at higher orders. This is because the effect that the corrections in $\bar{f}(t) = 1 - \frac{1}{(N+1)}t^{-1} + \ldots$ fades out with the order N is canceled out by the shrinking of the effective region of $\bar{f}_N(t)$. To suppress the correction, L^{th} order linear differential equation,

$$\prod_{i=1}^{L}\left[1 + p_i^{-1}\,(\mathrm{d}/\mathrm{d}\log t)\right]\bar{f}(t) = \bar{f}(\infty) + O\left(t^{-(L+1)}\right), \tag{2.16}$$

is effective to subtract the corrections. Here, p_i denotes the exponent of $\bar{f}(t)$

expanded at large t and $p_i = i$ $(i = 1, 2, 3, \ldots)$. We notice that the explicit expansion of $\bar{f}(t)$ at large t is not needed here. Used knowledge is just that the expansion is in the positive integer powers of $1/t$.

The left-hand side of (2.16) has small correction to $\bar{f}(\infty) = 1$ at large t of the order $O(t^{-(L+1)})$. Also at small t, the correction is expected to be reduced, since at large enough N, the coefficient of $t^{-(L+1)}$ vanishes as $(1/N)^{L+1}$ (see (2.4)). This suggests that $\bar{f}(t) \sim 1$ from large to small t region when N is large. We, therefore, replace $\bar{f}(t)$ in (2.16) by $\bar{f}_N(t)$, which is effective for small t provided that at some order or above $\bar{f}_N(t)$ may be a good simulation of $\bar{f}(t)$. Let us then denote

$$\psi_L = \prod_{i=1}^{L} \left[1 + p_i^{-1} \left(\mathrm{d}/\mathrm{d} \log t\right)\right] \bar{f}_N(t)\,. \tag{2.17}$$

By the input of exact values of p_i, we can indeed obtain better behaviors: See Fig. 1, where ψ_L for $L = 0, 1, 2, 3$ are plotted at $N = 20$. There appeared a plateau which grows flatter as the parameter numbers are increased. However, as the order N increases, the plateau becomes narrower and the center moves to the origin, which is the influence of the divergent nature of $1/M$ expansion. The plateau represents, due to the successful elimination of corrections, the leading term in the $t \to \infty$, $\bar{f}(\infty) = 1$. It is natural to estimate $\bar{f}(\infty)$ on the unique top on the plateau and this protocol is called the principle of minimum sensitivity (PMS) [7]. The results of estimation using PMS are summarized in Table I.

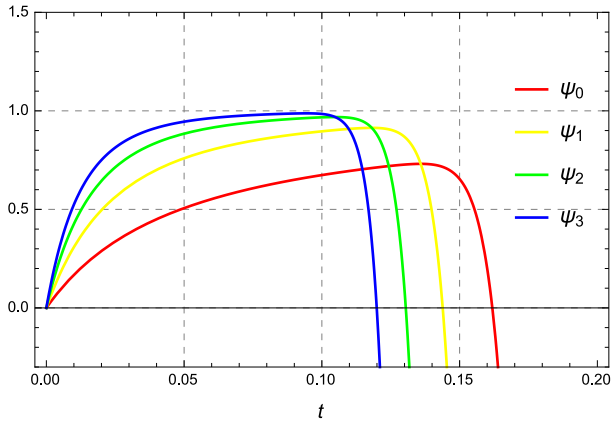


Fig. 1. 20^{th} order plots of $\psi_L(t) = \prod_{i=1}^{L}[1 + p_i^{-1}(\mathrm{d}/\mathrm{d}\log t)]\bar{f}_N(t)$ $(L = 0, 1, 2, 3)$ with the correct values $p_1 = 1$, $p_2 = 2$ and $p_3 = 3$.

TABLE I

The estimation of $f(0) = \bar{f}(\infty) = 1$ through $\psi_L(t)$ using the PMS. We performed computation to 300^{th} order, while the shown results are up to 40^{th}. The last row labeled "∞ (extrapolated)" indicates the extrapolated value from the 290^{th} and 300^{th} results via the Ansatz $\bar{f}(\infty)(1 - f_1 N^{-1})$.

N	$L = 0$	$L = 1$	$L = 2$
10	0.69276626	0.87951576	0.94485674
20	0.73101017	0.91367909	0.96853507
30	0.74556188	0.92559505	0.97580002
40	0.75337822	0.93172054	0.97928804
∞ (extrapolated)	0.78151	0.95212	0.98950
N	$L = 3$	$L = 4$	$L = 5$
10	0.97185783	0.98441767	0.99080598
20	0.98733751	0.99448001	0.99742866
30	0.99141838	0.99672795	0.99867246
40	0.99321942	0.99763006	0.99912290
∞ (extrapolated)	0.99771	0.99950	0.99989

The sequence of $L \geq 1$ exhibits remarkable improvement over the plane $L = 0$ sequence. Since many exponents are incorporated as the parameters of ψ_L, the accuracy becomes higher at all orders. However, the convergence issue is subtle up to the 300^{th} order which is the highest order estimation we have performed. To settle the issue, we have done the fitting assumed the Ansatz, $\bar{f}(\infty)(1 - f_1 N^{-1})$. From the sample at $N = 290$ and 300, which are the highest computation orders, we obtained the extrapolated values listed in Table I. In Fig. 2, we have shown the plots of the estimated sequence at $L = 1, 2, 3$ and the obtained fitted lines. It is confirmed that, at $L = 0 \sim 5$, though larger L provides better and accurate approximation, the limits extrapolated do not agree with the exact value $\bar{f}(\infty) = 1$. The origin of this discrepancy is again the divergent nature of $f(M)$ in $1/M$ expansion, which reflects the narrowness and movement to the origin of the plateau and the top of the plateau fails to attain to the height of $\bar{f}(\infty) = 1$.

The features described so far can be explained analytically as follows: First, let us consider the asymptotic behavior of the PMS solution t^* in the $N \to \infty$ limit. From numerical analysis, we find that t^* decreases as $t^* \sim c_L/N$ with c_L constant. The values of c_L are $c_0 \sim 3.4855$, $c_1 \sim 3.4252$, $c_2 \sim 3.3698$ and so on. Though these values are obtained at each L with respective highest-order (300^{th}) values of t^*, they are, in fact, dependent on N. Since the behaviors of the sequences of $t^* \times N$ to the order of $N = 300$ are monotonically increasing with N for all L examined, the values of c_L indicated in the $N \to \infty$ limit would be slightly larger than the above

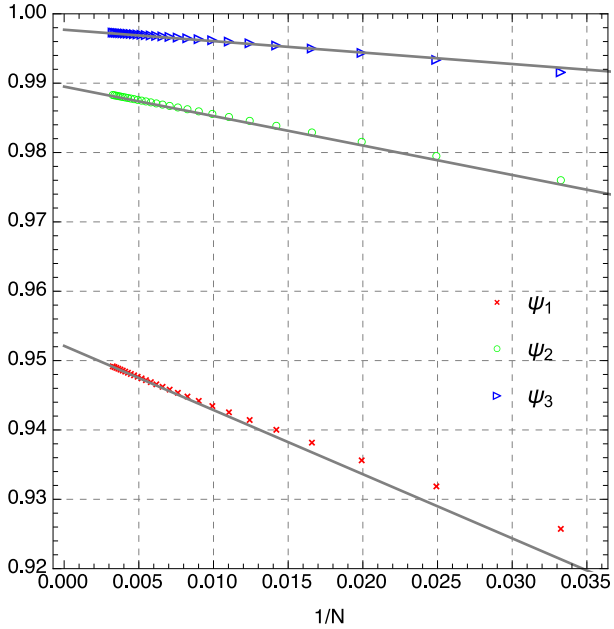


Fig. 2. Plots of estimation sequence *vs.* $1/N$ for $L = 1, 2, 3$. The solid gray lines represent the fitted lines obtained via the Ansatz $\bar{f}(\infty)(1 - f_1 N^{-1})$ from the results at 290^{th} and 300^{th}.

values. We can actually infer the value of true c_L to be identified only in the $N \to \infty$ limit from (2.15). For example, consider the case $L = 0$. The residual part R_N is given by

$$R_N = \bar{f}(t) - \bar{f}_N(t) = N!(-t)^N e^{-1/t}. \tag{2.18}$$

Substituting the Ansatz $t^* = c_0/N$ into the above, we obtain $R_N = N!$ $(-c_0/N)^N e^{-N/c_0}$ and at large enough N, from Stirling's formula, $R_N \sim \sqrt{2\pi N}(-c_0/e^{(1+1/c_0)})^N$. Thus, if $R_M(t^*) \to 0$ as $N \to \infty$, the condition $c_0/e^{(1+1/c_0)} < 1$ is deduced. The maximally allowed value of $c_0 = c_{0,\max}$ is then found as the solution of $\log c_{0,\max} = 1 + 1/c_{0,\max}$, giving $c_{0,\max} = 3.591121476668622\ldots$ For $L \geq 1$, the same analysis can be carried through and the result of upper limit of c_L is found to be independent of L. Thus, we conclude

$$c_{L,\max} = 3.591121476668622\ldots \tag{2.19}$$

The values of c_L for $L = 1 \sim 5$ obtained at $N = 300$ are all under and close to the above limit. Now as mentioned before, the estimated c_L grows with the order and surely tends to the value very close or exact to $c_{L,\max}$ at $L = 0, 1, 2, \ldots 5$. We hence assume that estimated c_L converges to $c_{L,\max}$ and

compute the limit of the sequence of $\bar{f}^*$. First of all, we note that $\bar{f}(t)$ can be used in this study instead of $\bar{f}_N$ itself since $R_N \to 0$ $(N \to \infty)$ is assured. Then, substituting $t = c_L/N$ into $\psi_L = N! \sum_{n=0}^{\infty} (-1)^n / \{(N+n)! t^n\}$ and expanding the result in $1/N$, we obtain

$$\psi_L(t^*) = 1 - \frac{1}{(1+c_L)^L} + O(1/N)\,. \tag{2.20}$$

Substitution of $c_{L,\max}$ into c_L produces

$$\lim_{N\to\infty} \psi_L(t^*) = 1 - \frac{1}{(1+3.591121476668622\ldots)^L}\,. \tag{2.21}$$

One finds that the above result agrees with the corresponding result indicated by "∞ (extrapolated)" in the last row in Table I.

The use of the exact values of the exponent is possible only when we know what values they are. In the realistic physical situation in the field of theoretic and statistical models, the exponents are not exactly known, of course. In this case, one approach is to resort to extended principle of minimum sensitivity, where the exponents are fixed so as to make the higher order derivatives of ψ_L be zero at the estimation point t^* [2–4]. In the present example, however, the approach fails. It is because the higher order derivatives themselves do not reach enough scaling behaviors.

2.4. Estimation via Padé approximant

As the second approach, we attempt another extrapolation scheme by the Padé method [8]. Padé approximants approximate a given function by the ratio of two polynomials in accordance with the truncated Taylor series.

Here, we utilize Padé approximants constructed from the series $\bar{f}_N(t)$. It should be reminded here that for the estimation of $f(0) = \bar{f}(\infty)$, the best Padé approximant among entries in Padé table is the diagonal one at even N, since we can take the limit $t \to \infty$ and the result directly provides the estimation of $\bar{f}(\infty) = 1$. To define the protocol clearly, let us denote the Padé approximant of $N = \rho + \tau$ decomposition as $\bar{f}_N[\rho/\tau]$. Here, the degree of the numerator polynomial is equal or less than ρ and the degree of the denominator polynomial is equal or less than τ. The estimate via diagonal approximant with even N is defined by

$$\bar{f}(\infty) = \lim_{t\to\infty} \bar{f}_N[\rho/\rho]\,, \qquad \rho = N/2\,. \tag{2.22}$$

For example, at $N = 10$,

$$\bar{f}_N[5/5] = \frac{10t + 160t^2 + 1470t^3 + 6960t^4 + 15240t^5}{1 + 25t + 300t^2 + 2100t^3 + 8400t^4 + 15120t^5} \tag{2.23}$$

and

$$\lim_{t\to\infty} \bar{f}_N[5/5] = \frac{127}{126} = 1.0079365079\ldots \tag{2.24}$$

The same method is also used for $f_N(M)$, the original truncated series. We estimated in the cases $(\rho,\tau) = (5,5),(10,10),(15,15),(20,20),(25,25)$ for both $f_N(M)$ and $\bar{f}_N(t)$. The result is shown in Table II. It is clearly seen that for $f_N(M)$, the sequence is monotonically increasing and shows tendency of approaching to 1. Actually, we find from numerical work that the estimate at N^{th} order is given by $N/(N+2) = 1 - 2/N + \ldots$ The convergence speed is thus slow. As for $\bar{f}_N(t)$, the convergence tendency is strongly exhibited and, in particular, the accuracy is excellent. We note that the sequence here shows small oscillation with the minimum period. At $N = 2+4K$ $(K = 0,1,2,\ldots)$, the sequence approaches to 1 from above and at $N = 4+4K$ from below. In each subsequences, the error is exponentially small with the N dependence roughly found to be $\log_e |f_N^* - 1| \sim 3.4 - 0.693 \times N$ for both subsequences (f_N^* denotes the estimate at the order N).

TABLE II

Estimation of $f(0) = \bar{f}(\infty) = 1$ using diagonal Padé approximants of $f_N(M)$ and $\bar{f}_N(t)$.

N	$f_N(M)$	$\bar{f}_N(t)$
10	0.8333333	1.0079365
20	0.9090909	0.9999891749
30	0.9375000	1.00000001289
40	0.9523809	0.99999999998549
50	0.9615385	1.0000000000000158

The reliability of results through diagonal approximants becomes solid when the near-diagonal ones, $\bar{f}_N[\rho/\tau]$ with $|\rho - \tau| = 1$ or 2, show broad plateaus. We have observed from orders $N \sim 30$ or larger, $\bar{f}_N[\frac{N}{2}+1/\frac{N}{2}-1]$ and $\bar{f}_N[\frac{N}{2}-1/\frac{N}{2}+1]$ for even N exhibit large plateaus. See the diagonal and near-diagonal Padé approximates in the plot (Fig. 3). The reference values from the near-diagonal approximants are obtained by the stationary values (local maximum in these cases) of $\bar{f}_N[\frac{N}{2}+1/\frac{N}{2}-1]$ and $\bar{f}_N[\frac{N}{2}-1/\frac{N}{2}+1]$. At $N = 34$, they are $0.9973217\ldots$ (at $t = 15.79656\ldots$) and $0.9973225\ldots$ (at $t = 15.80567\ldots$), respectively. These values are similar in accuracy to the estimates via ψ_4 case presented in the previous subsection.

At first sight, one might think that diagonal Padé approximants of $\psi_L = \prod_{i=1}^{L}[1+p_i^{-1}(\mathrm{d}/\mathrm{d}\log t)]\bar{f}_N(t)$ would be more suitable for $L = 1,2,3,\ldots$ Produced results are indeed accurate but not better than ψ_0. The reason may be found by the enumeration of zeros and poles of the diagonal Padé

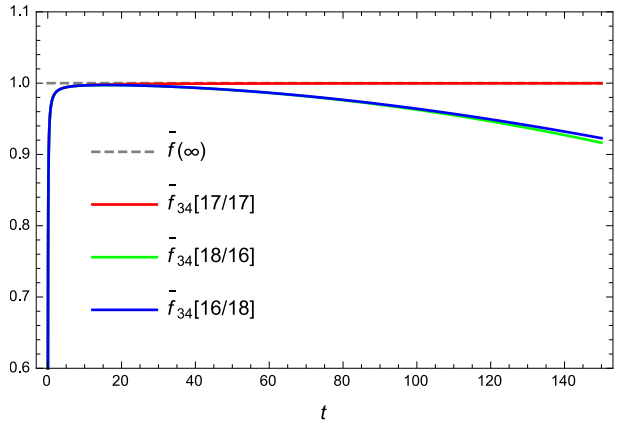


Fig. 3. Padé approximants $\bar{f}_{34}[17/17]$, $\bar{f}_{34}[18/16]$ and $\bar{f}_{34}[16/18]$.

approximants. The distribution of zeros and poles at $N = 30$ are depicted in Fig. 4. We see that for $\psi_0[15/15] = \bar{f}_N[15/15]$, the 8 poles in the left half-plane are approximately canceled by the zeros nearby them. On the other hand, for $\psi_1[15/15] = \{[1 + p_1^{-1}(\mathrm{d}/\mathrm{d}\log t)]\bar{f}_N\}[15/15]$, the approximate cancellation occurs for 6 pairs. Since the existence of bare poles would affect the behavior of diagonal Padé approximants on the positive real axis, it is better when the number of bare poles are small and located in remote place (the locations of poles of $\psi_1[15/15]$ are slightly inside of those of $\psi_0[15/15]$). We can thus roughly understand why $\psi_0[15/15]$ provides bet-

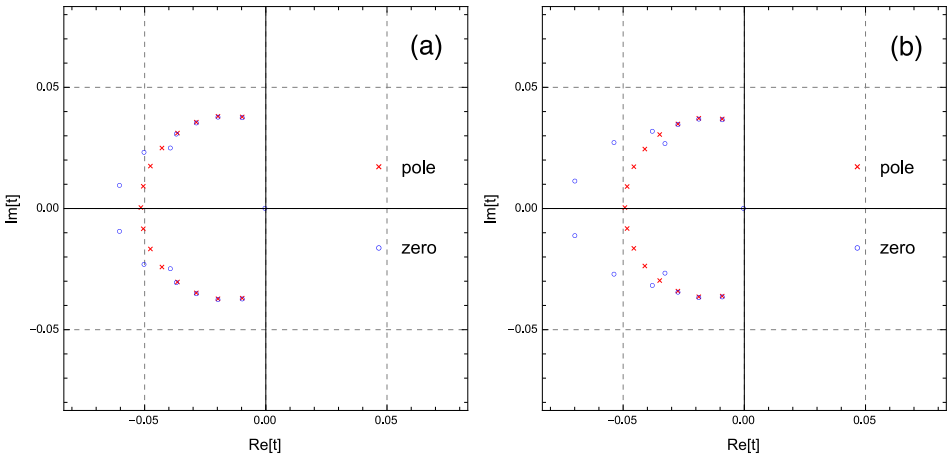


Fig. 4. Zeros and poles of Padé approximants (a) $\psi_0[15/15] = \bar{f}_{30}[15/15]$ and (b) $\psi_1[15/15]$.

ter estimation. Padé approximants of the same construction for $f_N(M)$, $\prod_{i=1}^{L}[1-p_i^{-1}(\mathrm{d}/\mathrm{d}\log M)]f_N(M)$, prove improvement for larger L. Actually, we have obtained analytic results of N^{th} order estimate inferred from numerical study that $N(N{+}6)/\{(N{+}2)(N{+}4)\}$ and $N(N^2{+}12N{+}44)/\{(N{+}2)(N+4)(N+6)\}$ for $L = 1$ and 2, respectively. The correction to 1 is respectively $O(1/N^2)$ and $O(1/N^3)$.

We now conclude that diagonal Padé approximants of $\bar{f}_N$ yield accurate convergent sequence of estimate.

3. Anharmonic oscillator

3.1. Perturbative expansion of the ground state energy

The perturbative ground state energy $E(m,\lambda)$ is given in the form of

$$E(m,\lambda) = m\sum_{n=0}^{\infty} a_n \left(\frac{\lambda}{m^3}\right)^n . \tag{3.1}$$

The coefficient a_n can be computed from the recursion technique due to Bender and Wu [9]. For instance, the first several coefficients read

$$a_0 = \frac{1}{2}\,, \qquad a_1 = \frac{3}{4}\,, \qquad a_2 = -\frac{21}{8}\,, \qquad a_3 = \frac{333}{16}\,. \tag{3.2}$$

We have generated the first 300 coefficients exactly and use the result in the following studies.

It was shown in Ref. [9] that the coefficient grows with the order n as

$$a_n \sim -\frac{\sqrt{6}}{\pi^{3/2}}(-3)^n\Gamma(n+1/2)\,, \tag{3.3}$$

indicating zero convergence radius with the alternate coefficients. In this paper, we deal with the truncated series to N^{th} order perturbative expansion written as

$$E_N(m,\lambda) = m\sum_{n=0}^{N} a_n \left(\frac{\lambda}{m^3}\right)^n . \tag{3.4}$$

The perturbative truncation order means the number of included terms and it is matched to the parameter N involved in the generalized binomial factor (1.7).

3.2. Binomial transform and linear delta expansion

In accordance with the dilatation by the rescaling of the square of the mass $m^2 = (1-\delta)/t$, we describe the perturbative series in terms of x defined by

$$x = \frac{\lambda^{2/3}}{m^2}\,. \tag{3.5}$$

The perturbative expansion is not a simple series expansion with positive integer powers but a singular expansion with fractional powers such as $x^{(3n-1)/2}$ $(n = 0, 1, 2, \ldots)$. With respect to such a singular series, the binomial transform is defined with (1.7) as

$$E_N(x,\lambda) = \lambda^{1/3}\sum_{n=0}^{N} a_n x^{(3n-1)/2} \to \lambda^{1/3}\sum_{n=0}^{N} \bar{a}_n t^{(3n-1)/2}\,, \tag{3.6}$$

where the coefficient $\bar{a}_n$ is given by

$$\bar{a}_n = a_n \binom{N}{\frac{3n-1}{2}} = a_n \frac{\Gamma(N+1)}{\Gamma\left(\frac{3n-1}{2}+1\right)\Gamma\left(N-\frac{3n-1}{2}+1\right)}\,. \tag{3.7}$$

That is, we obtain

$$\bar{E}_N(t) = \lambda^{1/3}\sum_{n=0}^{N} \bar{a}_n t^{(3n-1)/2}\,. \tag{3.8}$$

The generalized binomial transform possesses a few characteristic features which differ from the linear delta expansion as below: The first is that the factor $1/\Gamma(N-\frac{3n-1}{2}+1)$ becomes zero for some values of N (≥ 3) and n. It vanishes for $(N,n) = (3,3), (5,5), (6,5), (7,7), (8,7), (9,7), (9,9)$ and so on. This induces that a subset of terms in the original expansion is eliminated. Second, the factor takes negative values for various sets of (N,n) such as $(N,n) = (4,4), (6,6), (7,6), (8,8), (9,8)$ and so on. The negative binomial factor changes the sign of the coefficients and rigorous alternativeness is slightly broken. The original series is modified in this manner.

In contrast, the linear delta expansion does not change the sign. Some explanation would be needed here: Let us denote the result of linear delta-expansion be

$$E_{\mathrm{LDE},N}(m) = \lambda^{1/3}\sum_{n=1}^{N} a_n C_{N,n}\left(\lambda^{2/3}/m^2\right)^{(3n-1)/2}\,. \tag{3.9}$$

Here, we remind that the factor $C_{N,n}$ representing the modification comes from the term $m(\lambda/m^3)^n$ through the linear delta-expansion. One can obtain

$C_{N,n}$ from the plain perturbative series (3.1) by the shifts $\lambda \to \lambda\delta$ and $m^2 \to m^2(1-\delta)$. Then, $m(\lambda/m^3)^n \to m(\lambda/m^3)^n\delta^n(1-\delta)^{-(3n-1)/2}$. The expansion of $\delta^n(1-\delta)^{-(3n-1)/2}$ in δ to the order N and setting $\delta = 1$ gives $C_{N,n}$. For example, at $n = 0$, we shall expand it such that $(1-\delta)^{1/2} = 1 - \frac{1}{2}\delta - \sum_{k=1}^{N} \frac{(2k-1)!}{2^{2k-1}k!(k-1)!}\delta^k$. Then, putting $\delta = 1$, the summation of the resulting series gives $C_{N,0} = (2N)!/\{2^{2N}(N!)^2\}$. For general N, $C_{N,n}$ is obtained explicitly as [10]

$$C_{N,n} = \binom{N + \frac{n-1}{2}}{\frac{3n-1}{2}} = \frac{\Gamma\left(N + \frac{n+1}{2}\right)}{\Gamma\left(\frac{3n+1}{2}\right)\Gamma(N-n+1)}\,. \tag{3.10}$$

As may be clear from the above procedure, the result ensures that $C_{N,n} > 0$ at any finite order N for all $n = 0, 1, 2, \ldots, N$. We note that the factor $C_{N,n}$ is a rational number. On the other hand, $\binom{N}{(3n-1)/2}$ multiplied to the original expansion coefficient in the binomial transform includes π for odd n.

For further quantitative comparison, we have plotted the ratio $R_{N,n} = \binom{N}{(3n-1)/2}/C_{N,n}$ for $n = 0, 1, 2$ and 3 against N in Fig. 5. The ratio converges to unity in the $N \to \infty$ limit as $R_{N,n} = 1-(n-1)(3n-1)/N+O(N^{-2})$, but the difference is not negligible at finite orders except for $n = 1$ ($R_{N,1} = 1$ to all orders).

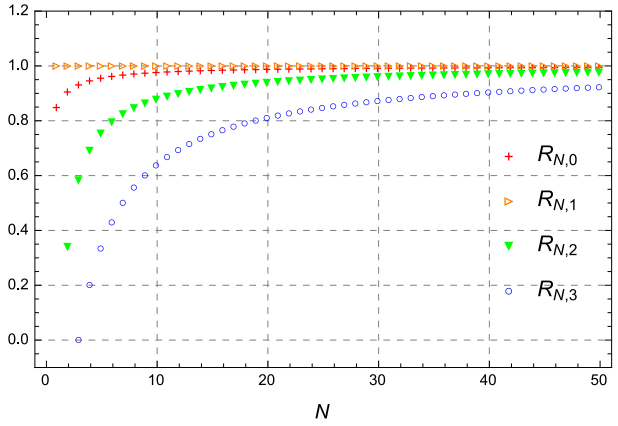


Fig. 5. Ratio plot of the leading and next-to-the leading order coefficients $R_{N,n} = \binom{N}{(3n-1)/2}/C_{N,n}$ for $n = 0, 1, 2, 3$.

The convergence in the linear delta expansion is proved in Ref. [11]. As for the generalized binomial transform method, the proof is not obtained. However, large order numerical study provides convincing affirmative result on the convergence issue under PMS protocol by the comparison with the results of sequence in the linear delta expansion.

3.3. Computation of the ground state energy

We now use $\bar{E}_N(t)$ to estimate the massless limit (or the strong coupling limit) of the ground state energy,

$$\lim_{m\to 0} E(m,\lambda) = \mathcal{E}\lambda^{1/3}\,, \tag{3.11}$$

where $\mathcal{E}$ is given by Vinette and Cizek [12] to the extreme accuracy [13],

$$\begin{aligned}\mathcal{E} \;=\; & 0.667986259155777108270962016919860199430404936984060455976660 8\,.\end{aligned} \tag{3.12}$$

Before explicit computation, let us see how binomial transformed energy behaves against t. Figure 6 shows the plot of $\bar{E}_N(t)$ at $N = 10, 20$ and 30. It is explicitly shown that $\bar{E}_N(t)$ clearly signals the correct value already at rather small order, around $N = 10$. The value to be identified as the estimate of $\mathcal{E}$ in the plotted curves are implied by the plateaus. The width of a plateau shrinks as the order grows and this feature reflects the asymptotic nature of the original perturbative series.

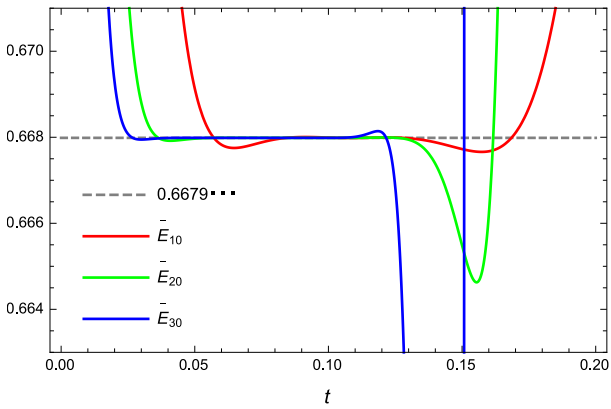


Fig. 6. Plot of $\bar{E}_N(t)$ with $\lambda = 1$ at $N = 10, 20$ and 30.

We notice then the problem pointed out by Neveu in [14] that the plateau exhibits a weak oscillation with tiny amplitudes. The oscillation may be embarrassing indeed, since it leads to the nonuniqueness of the stationary

solution under PMS protocol. In Ref. [4], Kneur, Neveu and Pinto proposed an interesting prescription to terminate this oscillation by introducing additional parameters in the linear delta expansion. Their idea is to generalize the simple prescription $m^2 \to m^2(1-\delta)$ to the one involving more parameters such as $m^2 \to m^2(1-\delta)(1+(a-1)\delta+\sum_{n=1} b_n\delta^{n+1})$ [15]. For example, at the second order, modification is to use the shift $m^2 \to m^2(1-\delta)(1+(a-1)\delta)$ and expand δ as in the conventional manner. It is possible to adjust a such that only single real-valued solution, the solution satisfying $(\partial/\partial m^2)E_{\mathrm{LDE},N} = (\partial/\partial m^2)^2 E_{\mathrm{LDE},N} = 0$ exists. At the third order, they found it suffice to use $m^2 \to m^2(1-\delta)(1+(a-1)\delta+b_1\delta^2)$ and seek the unique solution obeying $(\partial/\partial m^2)E_{\mathrm{LDE},N} = (\partial/\partial m^2)^2 E_{\mathrm{LDE},N} = (\partial/\partial m^2)^3 E_{\mathrm{LDE},N} = 0$ under the adjustment of a and b_1. The result was successful at low orders but turned out to getting worse at higher orders [4].

We like to remark on this problem that, without introducing additional parameters, even many oscillations occur and many candidates appear, the best optimal estimation point can be detected by carefully observing the derivatives of $\bar{E}_N$; See Fig. 7, where the first order derivative $\bar{E}_N^{(1)} = (\partial/\partial \log t)\bar{E}_N$ is plotted at $N = 23$ and 50. Seeing the plot, we find that there exists a narrow region within the plateau that the first order derivative is oscillating with smallest amplitude. With the increase of the order, the oscillatory wave becomes dense and a new oscillation wave seems to be born from the region, as signaled by the smallest amplitude of the first derivative. From this observation, we pose an assumption that the "center" of the set of zeros of $\bar{E}_N^{(1)}(t)$ is optimal as the estimation point. In the case shown in Fig. 7 (a),

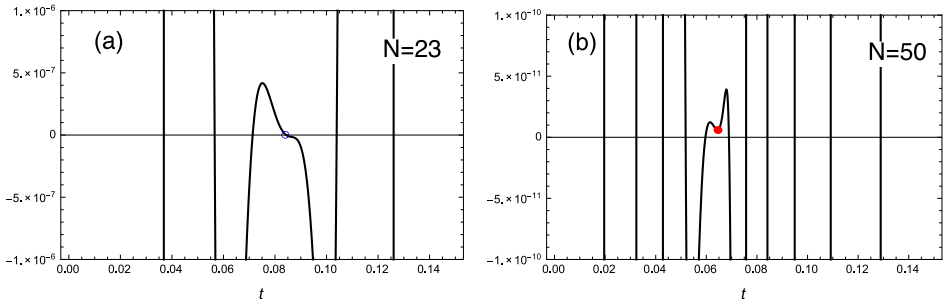


Fig. 7. First order derivatives $\bar{E}_N^{(1)}(t)$ at $N = 23$ and 50. Within the plotted range, $\bar{E}_{23}^{(1)}$ has 6 solutions and $\bar{E}_{50}^{(1)}$ has 11 solutions. Optimal stationary or almost stationary points are indicated by the open (blue) circle (23^{th}) and filled (red) circle (50^{th}) for the estimation of $\mathcal{E}$. At $N = 23$, the point is at $\bar{E}_N^{(1)} = 0$ and $|\bar{E}_N^{(2)}| \ll 1$. At $N = 50$, the point is at $|\bar{E}_N^{(1)}| \ll 1$ and $\bar{E}_N^{(2)} = 0$. The latter point corresponds to the reflection point with very small gradient.

it is natural that the point indicated by the open (blue) circle is optimal among other stationary points. In the case shown in Fig. 7 (b) on the other hand, the point indicated by the filled (red) circle exhibits the tendency in next few orders that it goes down and across the horizontal axis, creating a new stationary point. We, therefore, consider the black (red)-marked point should be regarded as the optimal estimation point, even though the first derivative is not zero at the point (note that the value of the first derivative is extremely small there in magnitude).

It is interesting to consider the complex extension of $\bar{E}_N(t)$ denoted as $\bar{E}_N(z)$ $(z \in \mathbb{C})$, where $z = t^{3/2}$. Numerically solving $\bar{E}_N^{(1)}(z) = 0$ at $N = 50$, we have plotted the solutions in the z-plane with open (blue) circles in Fig. 8. Filled (red) circles indicate the solutions of $\bar{E}_N^{(2)}(z) = [(\partial/\partial \log t)^2 \bar{E}_N]_{t\to z} = 0$. Now, the point is that there exists a small area in which the arc-shaped sequence of complex zeros and the set of real zeros on the positive real axis intersect. As the order increases, the numbers of stationary points in each sets increase and the intersection area becomes a dense set of zeros, which we call the center of zeros. The function is smoothest there and the amplitude is smallest. The two points indicated in Fig. 7 (a), (b) are located at this intersection area. The filled (red) circle indicated by the arrow in Fig. 8 is the filled (red) circle plotted in Fig. 7 (b).

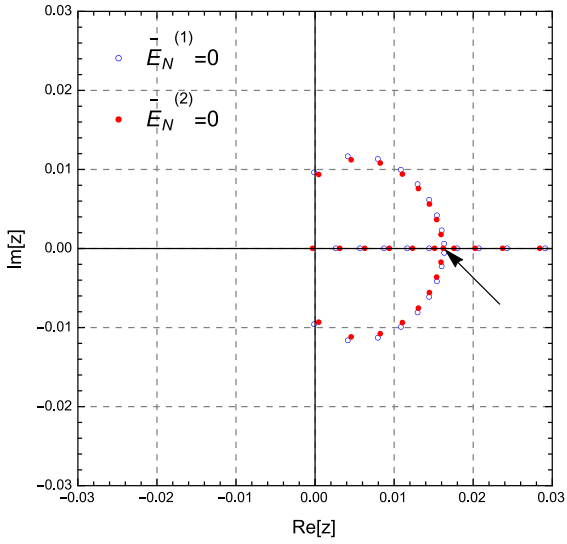


Fig. 8. The plot of zeros of the first and second order derivatives $\bar{E}_N^{(i)}(z)$ $(i = 1, 2)$ at $N = 50$ in the plane $z = t^{3/2} \in \mathbb{C}$. The open (blue) circles indicate zeros of $\bar{E}_N^{(1)}(z)$ and filled (red) circles zeros of $\bar{E}_N^{(2)}(z)$. We take zero of $\bar{E}_N^{(2)}(z)$ indicated by the arrow as the best optimal solution. This solution corresponds to the filled (red) circle shown in Fig. 7 (b).

These observations help us handling PMS in the complicated proliferation of stationary or almost stationary points. To summarize, pick out the point in the center of zeros satisfying either *(i)* $\bar{E}_N^{(1)}(t) = 0$ with $|\bar{E}_N^{(2)}(t)| \ll 1$ or *(ii)* $\bar{E}_N^{(2)}(t) = 0$ with $|\bar{E}_N^{(1)}(t)| \ll 1$. This prescription may be regarded as a variant of the PMS criterion and we continue using the term PMS in what follows. Under the above criteria, we have estimated $\mathcal{E}$ to 300^{th} orders. The result of the estimation is plotted in Fig. 9 where the vertical axis labels $\log_{10}|E^* - \mathcal{E}|$.

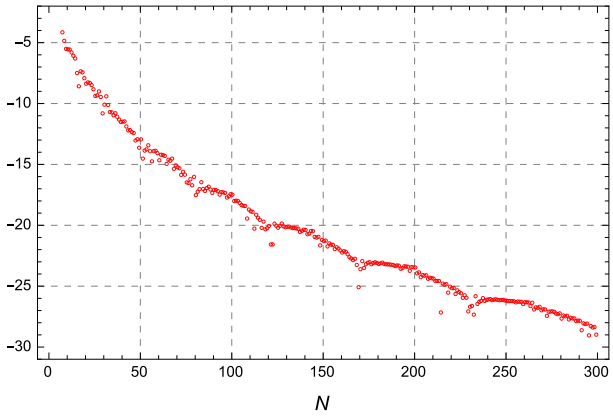


Fig. 9. Estimates of $\mathcal{E}$ up to 300^{th} orders. The vertical axis indicates $\log_{10}|E^* - \mathcal{E}|$, where E^* means the estimate.

We observe the expected growth of the accuracy with the orders. Due to the oscillation property of $\bar{E}_N(t)$, there is a periodic pattern and the length of the period becomes longer as the order increases. At the same time, the rate of accuracy growing gradually slows down, though there seems to be no limit of approaching to $\mathcal{E}$.

The effective region of $\bar{E}_N(t)$ shrinks as the order increases. This is already seen in Figs. 2, 3 and 4. Accordingly, the estimation point moves to the origin with the order. The value of the estimation point t^* is plotted in Fig. 10. The precise fitting of the data is not allowed since the distribution of data is somewhat complicated with periodic structure. We just remark that, from estimates for $N = 270 \sim 300$ where the data are rather steady, t^* tends to zero roughly like $\sim N^{-0.56}$.

3.4. Comparison with the linear delta expansion

In this subsection, we compare the result obtained in the generalized binomial transform with the one obtained in the linear delta expansion. The computation of the ground state energy in linear delta expansion has been

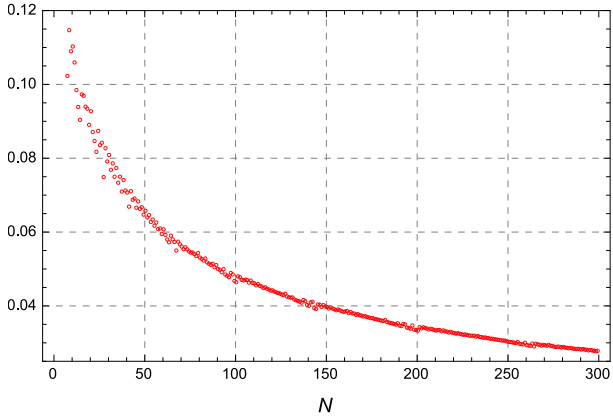


Fig. 10. Plots of the value of $t = t^*$ at which $\mathcal{E}$ is estimated.

already done by Janke and Kleinert up to 251$^{\text{th}}$ order [16] (the expansion technique is called the variational perturbation theory). Let us first explain the work with focusing on the related part.

The PMS criterion works more straightforwardly in the linear delta expansion. This is understood by plotting the function $E_{\text{LDE},N}(m)$ (see (3.9)). Omitting the graph plots, we note that the best estimation point given as the stationary point or the inflection point is always the one *at the largest value of* λ/m^3, since the oscillation amplitude becomes smallest there. It is interesting to see the distribution of zeros in the complex extension of the first order derivative $E^{(1)}_{\text{LDE},N}(z) = [(\partial/\partial \log m^{-2})E_{\text{LDE},N}]|_{\lambda/m^3 \to z}$, where $z = \lambda/m^3$. From the plot shown in Fig. 11, we find that the intersection of the zero point set on the positive real axis and the set extending in arc-form on the right half-plane occurs at the largest real zero (the point indicated by the arrow in Fig. 11). Thus, also in the linear delta expansion, the estimation point lies on the intersection of the two sets.

The estimation result at the largest stationary point is plotted in Fig. 12 and the numerical results in both schemes (linear delta and binomial) are tabulated in Table III. In Ref. [16], the highest order studied is 251$^{\text{th}}$ and the result is quoted as $\mathcal{E} = 0.66798625915577710827096$, which is confirmed by us with the explained protocol.

In Fig. 12, we have also plotted the results in generalized binomial transform for the sake of the comparison. At low orders up to, say roughly 20$^{\text{th}}$, the result from linear delta expansion is slightly more accurate. Then, as the order increases, the crossover occurs and at large orders, the results from binomial transform become superior. Since the sequence in binomial scheme achieves higher accuracy than the sequence (which convergence is proved) from linear delta expansion, its convergence is now verified.

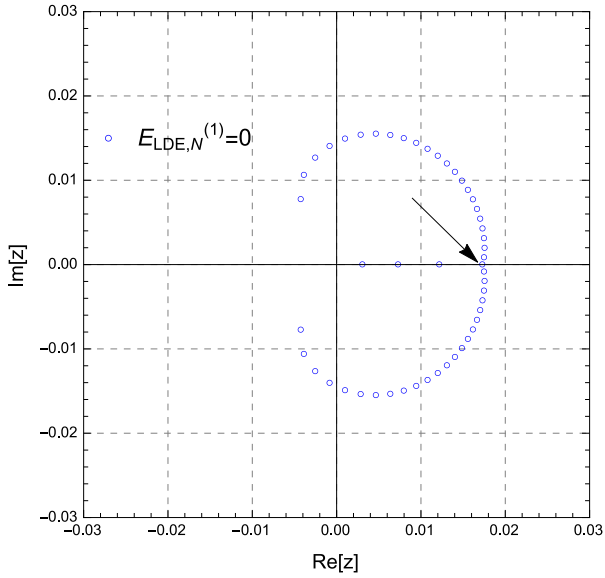


Fig. 11. The plots of zeros of the first derivative $\bar{E}^{(1)}_{\mathrm{LDE},N}(z)$ at $N = 50$. Here, the argument z is the complex extension of λ/m^3.

TABLE III

Estimation of $\mathcal{E} = 0.667986259155777108270962016919860199430404936\ldots$ in sample orders in linear delta expansion and generalized binomial transform approaches. The exact figures in each digits are written in Roman style, while figures in the last two digits including errors are written in slanted style.

N	Linear delta expansion	Generalized binomial transform
10	0.667985*57*	0.667983*37*
15	0.667986*30*	0.667985*58*
20	0.6679862*62*	0.6679862*68*
25	0.667986259*20*	0.667986257*9*
50	0.667986259155*92*	0.66798625915*758*
100	0.667986259155777*05*	0.66798625915577710*53*
150	0.667986259155777108*39*	0.667986259155777108271*4*
200	0.6679862591557771082703*4*	0.667986259155777108270959
250	0.667986259155777108270957	0.6679862591557771082709620*22*
300	0.66798625915577710827096248	0.667986259155777108270962016928

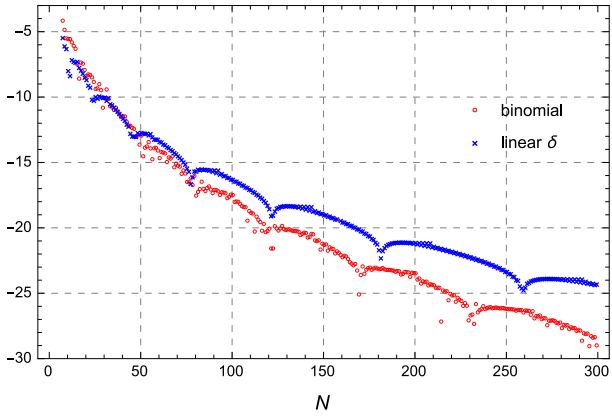


Fig. 12. The plots of $\log_{10}|E^* - \mathcal{E}|$ in the linear delta expansion and binomial transform.

In the case of the anharmonic oscillator, we have used no technique special to the model. The high accuracy of the estimation comes from the analytic structure with respect to m^2 of the strong coupling series of the ground state energy [17]

$$E(m,\lambda) = \mathcal{E}\lambda^{1/3}\left\{1 + e_1\left(m^2\lambda^{-2/3}\right) + e_2\left(m^2\lambda^{-2/3}\right)^2 + \ldots\right\}. \qquad (3.13)$$

Linear delta expansion eliminates lower order terms since $\{m^2(1-\delta)\}^L = 0$ for $N \geq L$. Also in binomial method, $\mathcal{B}_N[(m^2)^L] = \binom{N}{-L}t^L = 0$ since $\binom{N}{-L} = \Gamma(N)/\{\Gamma(-L+1)\Gamma(N+L+1)\} = 0$ for $L = 1, 2, 3, \ldots$ That is, both the linear delta expansion and binomial transform methods receive an advantage from the fact that $(m^2)^n \to 0$ $(n = 1, 2, 3, \ldots)$ after the expansion or transformation. This is the reason why linear delta expansion and binomial transform with respect to $m^2\lambda^{-2/3}$ yield accurate estimates unlike the case of Laplace integral where corrections of power series in $1/t$ remain.

3.5. Estimation of the strong coupling coefficients

Analyticity with respect to m^2 expressed in (3.13) can be numerically confirmed by binomial transform, as we can see below: Assume that there are fractional power-like terms and let the leading one be $\text{const} \times (m^2/\lambda^{2/3})^{\Delta}$ $(\Delta > 0)$. Then,

$$\mathcal{B}[E(m,\lambda)] = \mathcal{E}\lambda^{1/3}\left\{1 + \text{const} \times t^{-\Delta} + \ldots\right\}. \qquad (3.14)$$

The leading correction from $t^{-\Delta}$ must then be observed in $\bar{E}_N(t,\lambda)$ if it would exist, as would be seen in the plot of ψ_0 in Fig. 1 where t^{-1} correction

is active. But the numerical plot shown in Fig. 6 does not imply any power-like correction. This means that the terms of fractional powers are absent in the strong coupling expansion. Thus, expansion (3.13) is ensured even in our numerical study.

The coefficient $\alpha_k = \mathcal{E}e_k$ of the series (3.13) can be estimated in the following way: As the first example, we illustrate the estimation of α_1. Setting $\lambda = 1$, consider the derivative of $E(m^2, 1)$ with respect to m^2 denoted as $\partial E(m^2, 1)/\partial m^2 := E^{'}(m^2, 1)$. We obtain at small m^2

$$E^{'}(m, 1) = \alpha_1 + 2\alpha_2 m^2 + 3\alpha_3 \left(m^2\right)^2 \ldots \tag{3.15}$$

and at large m^2

$$E^{'}_N(m, 1) = \sum_{n=0}^{N} a_n \left(-\frac{3n-1}{2}\right) \left(1/m^2\right)^{(3n+1)/2} . \tag{3.16}$$

Then, the binomial transform eliminates corrections of integer powers of m^2 in (3.13) and may simply leave

$$\mathcal{B}\left[E^{'}(m, 1)\right] \sim \alpha_1 \tag{3.17}$$

at a certain region where (3.17) is expected to be recovered by $\mathcal{B}[E^{'}_N(m, 1)]$. As in the same manner of estimating $\mathcal{E}$, we have carried out estimation of α_1 by substituting

$$\mathcal{B}\left[E^{'}_N(m, 1)\right] = \sum_{n=0}^{N} a_n \left(-\frac{3n-1}{2}\right) \binom{N}{\frac{3n+1}{2}} t^{(3n+1)/2} \tag{3.18}$$

into $\mathcal{B}[E^{'}(m, 1)]$ and using PMS to pick out the optimal solution for α_1. For higher order coefficients, using the derivatives of $E(m^2, 1)$ with respective m^2, we can estimate α_2, α_3 and so on. We tabulate the results in Table IV. Having compared our results at $N = 250$ and 300, we consider that the figures at $N = 250$ to 10^{-24} order are correct for α_k $(k = 1, 2, 3, 4, 5)$.

Let us compare our results with those obtained by Janke and Kleinert at the order $N = 251$ [16]. Their results are:

$$\begin{aligned}
\alpha_1^{\mathrm{JK}} &= 0.1436687833808649100203\,, \\
\alpha_2^{\mathrm{JK}} &= -0.008627565680802279128\,, \\
\alpha_3^{\mathrm{JK}} &= 0.000818208905756349543\,, \\
\alpha_4^{\mathrm{JK}} &= -0.000082429217130077221\,, \\
\alpha_5^{\mathrm{JK}} &= 0.000008069494235040966\,.
\end{aligned} \tag{3.19}$$

TABLE IV

Estimation results of coefficients $\alpha_k = \mathcal{E}e_k$ $(k = 1, 2, 3, 4, 5)$ of the strong coupling expansion of the ground state energy at 250^{th} and 300^{th} orders. The results are expressed to the digit of the order of 10^{-28} the same order of correct $\mathcal{E}$ estimated at $N = 300$ (*cf.* Table III).

$\alpha_1\,(N = 250)$	0.14366878338086491002031908 08
$\alpha_2\,(N = 250)$	−0.00862756568080227912796357 44
$\alpha_3\,(N = 250)$	0.00081820890575634954241515 82
$\alpha_4\,(N = 250)$	−0.00008242921713007721991096 68
$\alpha_5\,(N = 250)$	0.00000806949423504096475447 89
$\alpha_1\,(N = 300)$	0.14366878338086491002031912 72
$\alpha_2\,(N = 300)$	−0.00862756568080227912796374 61
$\alpha_3\,(N = 300)$	0.00081820890575634954241559 47
$\alpha_4\,(N = 300)$	−0.00008242921713007721991189 49
$\alpha_5\,(N = 300)$	0.00000806949423504096475601 81

As in the case of $\mathcal{E}$, our results for α_k $(k = 1, 2, 3, 4, 5)$ are more accurate than α_k^{JK} by about $2 \sim 3$ digits. We thus conclude that, as long as the order is high, the estimate of strong coupling coefficients is better in binomial transform.

3.6. Binomial transform with respect to λ

The computation of the ground state energy has so far been done by taking the energy as a function of m^2. We investigate here the transform with respect to the coupling constant by taking the energy as a function of λ. In this point of view, the corrections have fractional powers in the strong coupling region as seen from (3.13). Hence, we can test the flexibility of the generalized binomial transform approach by the application to such a complicated case. To dilate the region around the strong coupling limit $\lambda = \infty$, we rescale $\lambda = g/(1-\delta)$ and expand the energy function in δ to the relevant order of perturbation series.

For the sake of notational simplicity, we set $m^2 = 1$. Then, the behavior of $E(1, \lambda)$ at $\lambda \gg 1$ reads from (3.13)

$$E(1,\lambda) = \mathcal{E}\lambda^{1/3}\left(1 + e_1\lambda^{-2/3} + e_2\lambda^{-4/3} + \ldots\right), \tag{3.20}$$

and at $\lambda \ll 1$

$$E_N(1,\lambda) = a_0 + a_1\lambda + a_2\lambda^2 + \ldots + a_N\lambda^N. \tag{3.21}$$

We investigate the computation of $\mathcal{E}$ in most part without using the values of the exponents of the corrections to the asymptotic term. We thus start

with

$$E(1,\lambda) = \mathcal{E}\left(\lambda^{1/3} + e_1\lambda^{-\theta_1} + e_2\lambda^{-\theta_2} + \dots\right). \tag{3.22}$$

The basic result needed for the transform is then

$$\mathcal{B}[\lambda^s] = \binom{N}{s} g^s. \tag{3.23}$$

Although the transform improves the simulation task of $\bar{E}(1,g)$ via $\bar{E}_N(1,g)$, to achieve a good accuracy, we need to reduce the correction. So we must somehow estimate first the values of the exponents θ_i up to, say, a first few i. It has turned out, though, that higher order θ_i is difficult to estimate precisely in stable and systematic manner. Here, we suffice ourselves with the reduction of the first order correction by the estimation of $\theta_1 = 1/3$ and make use of the result for the estimation of $\mathcal{E}$.

We start with noting that, since the leading order correction has the exponent $1/3$ known on dimensional grounds, the leading term can be eliminated in the following combination,

$$\bar{E} - 3\bar{E}^{(1)} = \mathcal{E}\left[e_1\binom{N}{\theta_1}(1+3\theta_1)g^{-\theta_1} + e_3\binom{N}{\theta_2}(1+3\theta_3)g^{-\theta_3} + \cdots\right], \tag{3.24}$$

with $\bar{E}^{(1)} = (\partial/\partial\log g)\bar{E}(1,g)$ understood. Here, we have used the fact that $\mathcal{B}_N[\lambda^{-\theta_2}] = \mathcal{B}_N[\lambda^{-1}] = 0$. Equally, all the terms with negative integer powers are eliminated by the binomial transform. To avoid notational complexity, we reparametrize exponents as $\theta_1(=1/3), \theta_2(=5/3), \theta_3(=7/3)$, $\theta_4(=11/3)$ *etc.* Then in general, it holds that

$$\prod_{i=0}^{L}\left[1 + \frac{1}{\theta_i}\frac{\partial}{\partial\log g}\right]\bar{E} = \text{const}\times g^{-\theta_{L+1}} + O\left(g^{-\theta_{L+2}}\right), \tag{3.25}$$

where $\theta_0 = -1/3$. Now, taking the following quotient and expanding it in $1/g$, we find

$$Q_L = \frac{\prod_{i=0}^{L}\left[1 + \frac{1}{\theta_i}\frac{\partial}{\partial\log g}\right]E^{(1)}}{\prod_{i=0}^{L}\left[1 + \frac{1}{\theta_i}\frac{\partial}{\partial\log g}\right]E} = -\theta_{L+1} + \dots, \tag{3.26}$$

where the dots mean the correction of the order of $O(g^{-\theta_{L+2}+\theta_{L+1}})$. We here concern the case of $L = 0$, giving at large g,

$$Q_0 = \frac{\left[1 - 3\frac{\partial}{\partial\log g}\right]E^{(1)}}{\left[1 - 3\frac{\partial}{\partial\log g}\right]E} = -\theta_1 + \dots \tag{3.27}$$

The quotient Q_0 is a divergent series in g which we denote as $Q_{0,N}$, where $\bar{E}_N$ and $\bar{E}_N^{(1)}$ are used in the places of $\bar{E}$ and $\bar{E}^{(1)}$. The function $Q_{0,N}$ thus defined looks like the Padé-type rational function but it is actually not. Hence, by first expanding $Q_{0,N} = [1 - 3\frac{\partial}{\partial \log g}]E_N^{(1)}/[1 - 3\frac{\partial}{\partial \log g}]E_N$ in g, we construct diagonal Padé approximants to circumvent the zero-convergence-radius difficulty. We then take the $g \to \infty$ limit of $Q_{0,N}[N/2, N/2]$ as the estimate of θ_1. That is, from (3.27),

$$\lim_{g\to\infty} Q_{0,N}[N/2, N/2] = -\theta_1 \,. \tag{3.28}$$

The result is plotted in Fig. 13 with the label "1p(opt-Pade)". The sequence does not exhibit clear shape and the convergence issue is not definitive. However, the estimation of θ_1 is accurate enough and we make use of the estimate at the order N to the estimate of $\mathcal{E}$ at the same order in the following manner.

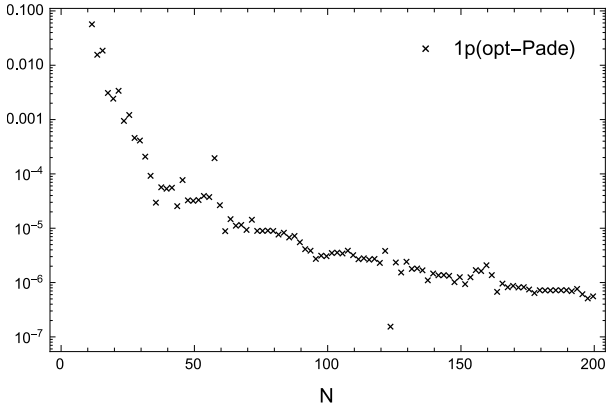


Fig. 13. The logarithmic plots of $|\theta_1 - 1/3|$ up to 200^{th} order.

One technical point to be payed attention is that the asymptotic of $\bar{E}$ in $g \to \infty$ is $\mathcal{E}\binom{N}{-1/3}g^{1/3}$ which is g-dependent. The ground state energy may be estimated in this case by dividing $\bar{E}$ by $\binom{N}{-1/3}g^{1/3}$. To improve the accuracy, however, we again use first order reduced function $[1 + (1/\theta_1)\partial/\partial \log g)]\bar{E}$. We thus study the combination $(\bar{E} + (1/\theta_1)\bar{E}^{(1)})/\{\binom{N}{-1/3}g^{1/3}\}$ which tends to $\mathcal{E}$ in the large g limit,

$$\lim_{g\to\infty} \frac{\bar{E} + \frac{1}{\theta_1}\bar{E}^{(1)}}{\binom{N}{-1/3}g^{1/3}} = \mathcal{E} \,. \tag{3.29}$$

Now, in the use of $\bar{E}_N$ and $\bar{E}_N^{(1)}$, the above limit does not hold even when we employ Padé approximants of any $[\rho/\tau]$ element in the numerator $\bar{E}_N+\frac{1}{\theta_1}\bar{E}_N^{(1)}$ of (3.29). This is reasonable since beyond narrow effective region of the series expansion Padé approximants take extrapolation affected by the highest orders g^ρ and g^τ of the numerator and the denominator, giving the behavior $(\bar{E}+\frac{1}{\theta_1}\bar{E}^{(1)})[\rho/\tau] \sim \text{const} \times g^{\rho-\tau}$, where the exponent cannot agree with $1/3$, the power of $g^{1/3}$. The expected asymptotic behavior $\sim g^{1/3}$ should occur at a certain region where g is not so large. The reliable region is indicated by the plateau in the combination (3.29) and the plateau serves an optimal estimation point of $\mathcal{E}$ under PMS. Due to the smallness of the exponent $1/3$ which should be recovered by Padé approximants, the best choice is the diagonal one. Then, we find that the optimal point occurs at either the extremum or the reflection points with small enough gradient. We also keep the estimate when poles on the positive real axis exist.

The result is plotted in Fig. 14 by the black cross labeled "1p(opt-Pade)". In Fig. 14, we have also plotted, for the comparison with the idealistic same optimization procedure, the result at the first and second order reductions of corrections with exact exponents. The "1p(exact-Pade)" labeled sequence shows the result via the quotient $[1+3(\partial/\partial\log g)]\bar{E}/\{\binom{N}{-1/3}g^{1/3}\}$ and the "2p(exact-Pade)" via the quotient $[1+3/5(\partial/\partial\log g)][1+3(\partial/\partial\log g)]$

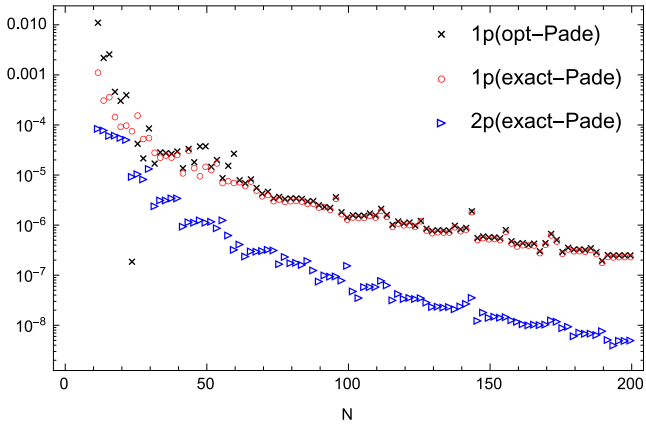


Fig. 14. The logarithmic plots of $|E^*-\mathcal{E}|$ up to 200^{th} order in the three methods: The "1p(opt-Pade)" shows the result from the first order reduction via $[1+3(\partial/\partial\log g)]\bar{E}/\{\binom{N}{-1/3}g^{1/3}\}$ with the order-dependent optimal θ_1. The "1p(exact-Pade)" sequence shows the result via $[1+3(\partial/\partial\log g)]\bar{E}/\{\binom{N}{-1/3}g^{1/3}\}$ with exact θ_1 and the "2p(exact-Pade)" via $[1+3/5(\partial/\partial\log g)][1+3(\partial/\partial\log g)]\bar{E}/\{\binom{N}{-1/3}g^{1/3}\}$ with exact θ_1 and θ_2.

$\bar{E}/\{\binom{N}{-1/3}g^{1/3}\}$. We now see that the optimal solution of θ_1 provides almost the same accuracy with the use of the exact value of θ_1. The reduced function exact to the second order brought more accuracy as it should.

From the plots, all the above three sequences to $N = 200$ appear to converge from the plots. One evidence of the convergence of the sequences comes from the behaviors of estimation point $g = g^*$. All three sequences of g^* show gradual increase with the order. This means that the approximate region is indeed extrapolated to larger g and, consequently, the convergence becomes quite conceivable due to the disappearance of the binomial coefficient of $g^{-\theta_i}$ $(i = 1, 2, 3, \ldots)$, $\binom{N}{-\theta_i}$, in the $N \to \infty$ limit.

The reduction of the correction provided by (3.25) gives further accurate estimates as the order of reduction L is increased. By using exact values of θ_i to many more orders, we obtain

$$L = 10 \ : \ 0.667986259155777108587259 91\,, \tag{3.30}$$

$$L = 20 \ : \ 0.667986259155777108271119 96\,, \tag{3.31}$$

$$L = 30 \ : \ 0.667986259155777108270962 68 \tag{3.32}$$

at $N = 250$. The results are respectively exact to 10^{-18}, 10^{-20} and 10^{-24} orders. The last result achieved the accuracy with the almost same order with the one in linear delta expansion. The case $L = 40$ gives less accurate result at $N = 250$ than the case of $L = 30$. However, we confirmed that at higher order $N = 300$, the case $L = 40$ exceeds in the accuracy than the case $L = 30$: error $= 1.8 \times 10^{-26}$ $(L = 30)$ and error $= 9.6 \times 10^{-27}$ $(L = 40)$. Thus, increasing the incorporated exponents indeed improves the accuracy while the effect manifests at larger orders.

4. Concluding remarks

We have explored the generalized binomial transform in the application to a Laplace integral and the quantum anharmonic oscillator in the perturbative framework. Let us summarize the investigation below.

In the Laplace integral function (2.5), binomial transform eliminated the logarithmic singularity at $M = 0$ and left the series in $1/t$. This is an advantage of the transformed series. The limit $\lim_{M\to 0+} f(M)$ is approximately computed from binomial transform of $f(M)$ expanded in $1/M$ valid at $M \gg 1$. Here, the use of the technique to subtract corrections in assumed power series was critical to achieve a good accuracy. The extrapolation to the infinite order by a simple fitting Ansatz predicts a slightly different value, which is caused by the nonconvergence nature of divergent series. To go beyond that difficulty, we found that diagonal Padé approximants of the transformed series provided excellent estimation at finite orders and solid evidence of convergence to the exact limit.

In the case of the anharmonic oscillator, the ground state energy computation is successful in the naive transformed function by detecting the optimal stationary or almost stationary points among many candidates under PMS. The presence of a few to many stationary points is not a serious drawback of binomial transform or linear delta expansion, since the optimal and best estimation comes from the point with the smallest amplitude and is thereby detectable. The accuracy of estimate is periodically improving as the order grows and the convergence of the sequence is confirmed by the comparison with that in the linear delta expansion. Also the coefficients in the strong coupling expansion could be estimated with the same level of accuracy. The high level of accuracy has its origin to the fact that the energy function $E(m^2, \lambda)$ is analytic around $m^2 = 0$ [17]. In this case, the subtractive-reduction of the corrections with PMS brings no essential improvement.

As the third study, from the point of view that the ground state energy is considered as a function of the coupling constant, we investigated the binomial transform approach to the computation of $\mathcal{E}$. Explicit reduction under the circumstance that θ_i is not known was carried out in the case of one-parameter (θ_1) reduction. Although the estimates became less precise compared with the previous two cases, obtained estimations were satisfactory. It has been explicitly confirmed that the subtractive-reduction to higher order corrections is effective to obtain accurate estimates. The problem is, of course, the precise values of the exponent θ_i is necessary. If there is no confluent singularity, it is expected that accurate results would be obtained with the aid of approximate elimination of higher order corrections. However, in models where a new singularity represented by the correction to the scaling exponent exists, the estimation with high accuracy may become a hard task, in particular, for divergent series.

In these three estimation tasks, we found that, when the transformed function has power-like corrections in the target region of the argument (the region where $M \ll 1$ in the present work), nonconvergent nature of divergent series available in the opposite accessible region does not allow the exact convergence of the sequence of estimates from transformed polynomial, though the improvement by the reduction of the correction produces accurate results. The problem has been resolved by the Padé approximant method by which the successful extrapolation beyond original narrow effective region was achieved. Note that, in the study of the anharmonic oscillator based on the binomial transform with respect to λ, reduction of the first order correction was crucial for the estimation by the Padé approximants. In various physical models, the combined use of the correction–reduction and Padé approximants may become useful tools for dealing with the divergent

series of a given function, usually accessible in the perturbative side where $M \gg 1$, for the quantitative computation of the function in the target region where $M \ll 1$.

REFERENCES

[1] H. Yamada, *Phys. Rev. D* **76**, 045007 (2007).

[2] H. Yamada, *Phys. Rev. E* **90**, 032139 (2014).

[3] H. Yamada, *Braz. J. Phys.* **45**, 584 (2015).

[4] J.-L. Kneur, A. Neveu, M.B. Pinto, *Phys. Rev. A* **69**, 053624 (2004) and the references therein.

[5] R. Seznec, J. Zinn-Justin, *J. Math. Phys.* **20**, 1398 (1979); J. Zinn-Justin, *Appl. Num. Math.* **60**, 1454 (2010) [arXiv:1001.0675 [math-ph]].

[6] A. Duncan, M. Moshe, *Phys. Lett. B* **215**, 352 (1988); A. Duncan, H.F. Jones, *Nucl. Phys. B* **320**, 189 (1989); I. Buckley, H.F. Jones, *Phys. Rev. D* **45**, 654 (1992); **45**, 2073 (1992); J. Akeyo, H.F. Jones, *Phys. Rev. D* **47**, 1668 (1993).

[7] P.M. Stevenson, *Phys. Rev. D* **23**, 2916 (1981); *Nucl. Phys. B* **203**, 472 (1982).

[8] G.A. Baker, Jr., P.R. Graves-Morris, *Padé Approximants*, 2nd edition, Cambridge University Press, 1996.

[9] C.M. Bender, T.T. Wu, *Phys. Rev.* **184**, 1231 (1969); *Phys. Rev. D* **7**, 1620 (1973).

[10] B. Bellet, P. Garcia, A. Neveu, *Int. J. Mod. Phys. A* **11**, 5587 (1996).

[11] R. Guida, K. Konishi, H. Suzuki, *Ann. Phys.* **241**, 152 (1995); **249**, 109 (1996).

[12] F. Vinette, J. Cizek, *J. Math. Phys.* **32**, 3392 (1991).

[13] Weniger also proposed a method admitting accurate computation of the ground state energy of the quartic, sextic and octic anharmonic oscillator. See E.J. Weniger, *Phys. Rev. Lett.* **77**, 2859 (1996).

[14] A. Neveu, *Nucl. Phys. B Proc. Suppl.* **18**, 242 (1990).

[15] However, this generalization complicates the concept of interpolation. The Hamiltonian becomes

$$H(\delta; a, b_n) = \frac{1}{2}\left(\frac{\partial\phi}{\partial q}\right)^2 + \frac{m^2}{2}(1-\delta)\left\{1 + (a-1)\delta + \sum_{n=1} b_n \delta^{n+1}\right\}\phi^2 + \delta\lambda\phi^4\,,$$

and the physical interpretation is obscured.

[16] W. Janke, H. Kleinert, *Phys. Rev. Lett.* **75**, 2787 (1995).

[17] B. Simon, *Ann. Phys. (N.Y.)* **58**, 76 (1970).